

He-Polymer Microchip Plasma (PMP) System Incorporating a Gas-Liquid Separator for the Determination of Chlorine Levels in a Sanitizer Liquid

Joosuck Oh, Y. H. Kim, and H. B. Lim*

Department of Chemistry, Dankook University, NSBT, Yongin, Gyeonggi 448-701, Korea

*E-mail: plasma@dankook.ac.kr; hblim@dku.edu

Received October 10, 2008, Accepted January 12, 2009

The authors describe an analytical method to determine total chlorine in a sanitizer liquid, incorporating a lab-made He-rf-plasma within a PDMS polymer microchip. Helium was used instead of Ar to produce a plasma to achieve efficient Cl excitation. A quartz tube 1 mm i.d. was embedded in the central channel of the polymer microchip to protect it from damage. Rotational temperature of the He-microchip plasma was in the range 1350-3600 K, as estimated from the spectrum of the OH radical. Chlorine was generated in a volatilization reaction vessel containing potassium permanganate in combination of sulfuric acid and then introduced into the polymer microchip plasma (PMP). Atomic emission lines of Cl at 438.2 nm and 837.7 nm were used for analysis; no emission was observed for Ar plasma. The achieved limit of detection was 0.81 $\mu\text{g mL}^{-1}$ (rf powers of 30-70 W), which was sensitive enough to analyze sanitizers that typically contained 100-200 $\mu\text{g mL}^{-1}$ of free chlorine in chlorinated water. This study demonstrates the usefulness of the devised PMP system in the food sciences and related industries.

Key Words: He plasma, Atomic emission, Determination of chlorine, Polymer microchip plasma

Introduction

Chlorinated water is used as a sanitizer for sterilizing various types of vegetables and foods, typically at concentrations of 100-200 $\mu\text{g/mL}$.¹⁻³ Since chlorine content directly influences sanitization efficiency, the determination of total chlorine provides useful control information. Unfortunately, the range of analytical methods available for this purpose is severely limited in terms of their practical applications. For example, ion chromatography (IC) is too sensitive and expensive to be used in the manufacturing line to detect such a high concentration. Plasma based methods, such as inductively coupled plasma atomic emission spectrometry (ICP-AES), can efficiently and selectively atomize chlorine and facilitate its analysis spectroscopically,⁴⁻⁶ but considerable energy is required to excite and ionize chlorine. Moreover, plasma based methods devised to date are expensive and do not meet the requirements of industrial users despite their sensitivities and reliabilities, and thus, smaller and more cost effective systems are required for production use. Various types of micro plasmas have been recently described, such as, CCP,⁷⁻⁹ MIP,^{4,10,11} ICP,^{12,13} and others, which can detect halogens. However, argon plasmas have insufficient energy to excite halogens,¹⁴ and thus, helium has been used instead due to the higher excitation and ionization energy. The thermal properties of plasmas can be estimated using several techniques, such as, mass spectrometry, Langmuir probe, and optical techniques.^{9,15-18} Furthermore, rotational temperatures of plasmas can be estimated from rotational temperatures of OH radical emission spectra and Boltzmann plotting.¹⁹

Even though the He plasma operates at high temperatures, water vapor entering the plasma with the chlorine can be problematic. Therefore, in the devised system, chlorine is dried before being introduced to the plasma. Various techniques are available to remove water vapor for the analysis of

metals, for example, hydride generation and cold vapor generation.²⁰ Recently, a method of generating gaseous halogens from halides by oxidation was reported for a He-microchip plasma-based method.⁴

Our laboratory has previously described Ar polymer microchip plasma (PMP) systems.²¹ In the present study, a He-PMP system with a gas-liquid separator and a reaction cell was built for the determination of chlorine in sanitizer solutions, with a view toward its usage for manufacturing process control in the food industry. The temperature of He plasmas was estimated by determining OH rotational temperatures and compared to those generated by Ar plasmas. Chlorine vapor was generated and dried in a gas-liquid separator that was composed of a reaction vessel and a condenser, then introduced into the He microchip plasma for excitation and spectroscopic analysis.

Experimental

Microchip plasma system. A lab-fabricated, PDMS microchip He-plasma with a high-resolution detection system was built, as shown in Fig. 1. The rf plasma was contained in a quartz tube (1 mm i.d. and 2 mm o.d.), which was embedded in the central channel (2 mm diameter, 50 mm long) of the PDMS polymer chip, as described in a recent article.²¹ In order to achieve Cl excitation, helium was used instead of argon, and thus the quartz tube was required to resist the higher temperatures generated by the He plasma than Ar plasmas.²² Emitted light was collected using an optical fiber (protected by a He flow of 300 mL min^{-1}) embedded at the downstream end of the channel, and then dispersed by a monochromator (0.70 m focal length, Model DM-700M, Dongwoo Optron, Korea) equipped with a photomultiplier tube (Hamamatsu photonics, Model R955) and a dual grating (1200 grooves/mm for a 750 nm blazed angle and 2400 groove

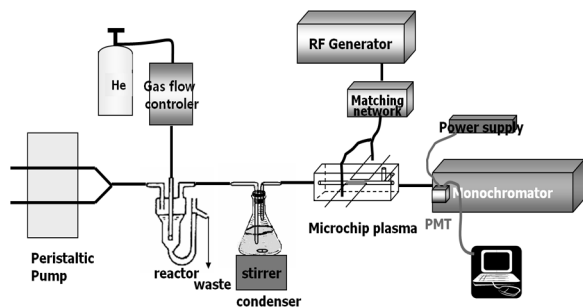


Figure 1. Schematic of the PDMS polymer He microchip plasma system with a gas-liquid separator.

Table 1. Optimized experimental conditions

He gas flow	About 0.5 L/min
Uptake rate for sample solution and oxidizing reagent	8 mL/min
RF power	60 W
PMT voltage	750 V
Slit width	100 μ m

for a 300nm blazed angle). Rf power was supplied at 15-70 W (13.56 MHz, Model PG-300A, Hwa Yong Tech., Korea) to the Cu electrodes to generate the plasma at a He gas flow of ca. 0.5 L min⁻¹, which was controlled using a ball type flow meter.

Sample introduction and measurement. The reaction vessel,⁴ in which chlorine is generated was made of Pyrex[®] glass, as shown in Fig. 1. Samples were reacted with a mixture of 10 mM KMnO₄ (Sigma-Aldrich 99%+A.C.S. reagent) and 9 M sulfuric acid (electronic grade, Dongwoo Finechem Co. Ltd), both were pumped into the reaction vessel using a peristaltic pump (Gilson, Miniplus 3). The chlorine gas so generated was passed in a He stream thru a glass frit of the reaction vessel. The chlorine gas was separated from the water vapor in the vessel and then dried in the condenser filled with concentrated sulfuric acid, and finally swept into the PMP by the helium nebulizer gas. KCl (first grade, Duksan Pharmaceutical Co., Ltd.) was dissolved in de-ionized water (18.2 M Ω , prepared by Milli-Q, Millipore) and used as a reference solution. The Cl emission lines used for analysis were at 438.2 nm and 837.7 nm.

The optimized experimental conditions used are summarized in Table 1. Because the oxidation reaction is rapid, the Cl peak rose from the baseline within a few seconds of adding a sample.

Results and Discussion

Rotational temperatures of OH radical in the He-polymer microchip plasma (PMP). Rotational temperature of plasmas was estimated using Boltzmann plots and the Q₁ branch from Q₁(2) to Q₁(14) in the 3075-3115 Å region of the OH radical. Figure 2 shows OH spectrum generated by the He-plasma. In order to reduce spectral interference, a high resolution monochromator was employed in this study.

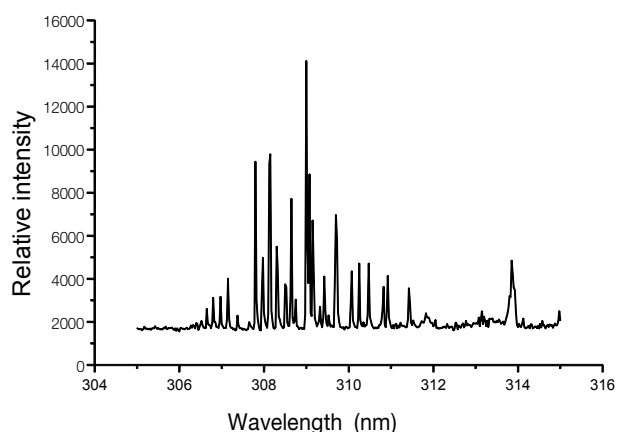


Figure 2. Emission spectrum of the OH molecule obtained from the He-PMP.

The following equation (1) was used to generate Boltzmann plots:

$$-\ln\left(\frac{I_{J'J''}}{S_{J'}v_{J'J''}^4}\right) = \alpha + B'J'(J'+1)\frac{1}{KT_{\text{rot}}}, \quad (1)$$

where, B'(J') is the rotational constant, $v_{J'J''}$ is the frequency of the rotational line, $S_{J'}$ is the emission line strength, $I_{J'J''}$ is the emission intensity of the (J'-J'') transition, and k is Boltzmann's constant. The line strength, $S_{J'}$, can be obtained from equation (2) using a value of 24.97 K for B'/k, which corresponds to the 2 Σ^+ state.¹⁸

$$S_{J'} = \frac{(2J'+1)}{4} \quad (2)$$

The rotational temperature was obtained by plotting $-\ln(I_{J'J''}/S_{J'}v_{J'J''}^4)$ versus the corresponding J(J+1) value of the emission band. As an example, a representative Boltzmann plot at an rf power of 15 W is shown in Fig. 3. As shown by the plot, the rotational temperature was split into two ranges, i.e., 'high' and 'low', depending on J(J+1) due to the non-equilibrium state of gas kinetic energy in the micro plasma. Measured temperatures ranged from 1780 K to 3710 K, which is both higher and narrower than that of the Ar plasma formed in a PDMS channel, i.e., 800-3200 K. For comparison purposes, the same operating conditions were used for the He-PMP and the Ar-PMP, although the He-PMP can operate at higher rf powers. The 'high' temperature was obtained at the lines of high excitation energy and showed relatively poor linear regression coefficient, R, because of its small emission intensity. This kind of a non-linear rotational distribution has been reported and discussed previously,⁹ and was found to correspond to the sum of two separate Boltzmann distributions.

Since the rotational temperature is dependent upon rf power, we studied the effect of rf power on this temperature; results are shown in Fig. 4. When rf power was increased from 15 to 40 W for the He-PMP at the same operating condition as for the Ar-PMP for comparison, both the estimated 'high' and 'low' gas temperatures decreased from 3710 to 3141 K and

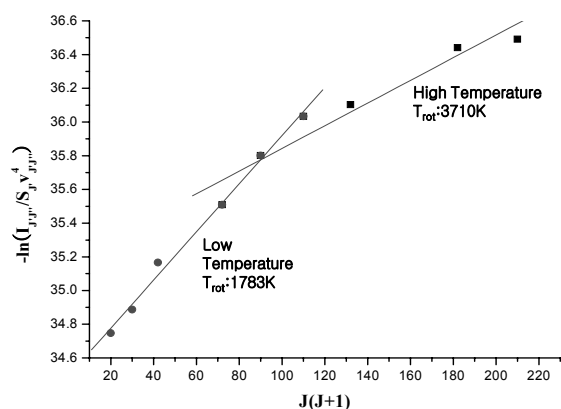


Figure 3. Boltzmann plot of the OH molecular band using the He-PMP at 15 W.

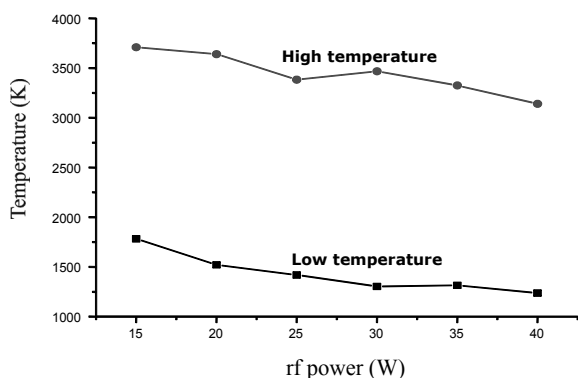


Figure 4. Relation between gas kinetic temperature and rf power supplied to the He-PMP.

from 1780 to 1240 K, respectively. Due to the higher temperature in the He-PMP, robustness to water loading and analytical performance for the detection of metal ions was expected to be improved, compared to the Ar plasma. In addition, it should be noted that the He-PMP is capable of operating at powers substantially higher than 40 W, and thus, it is likely to be more stable and robust than the Ar-PMP.

Measurement of Cl levels. As was expected the high ionization potential of He, 24.58 eV improved the emission intensity of Cl(I) at 12.96 eV. In fact, the He-PMP produced Cl emission that was strong enough to be detected in the low power range (30–70 W). Furthermore, because the quartz tube was inserted into the central channel of the PDMS polymer microchip, the He-PMP system can be operated at higher powers. However, the 30–70 W power range was adequate for our purposes for total chlorine levels of $\sim 10,000 \mu\text{g/mL}$.

Although various Cl(I) emission lines were examined for analytical purposes, i.e., 107.1 nm, 134.7 nm, 438.2 nm, 479.4 nm, 489.6 nm, and 837.7 nm, only at 438.2 nm and 837.7 nm were used because the sensitivities of the other lines were inadequate, as is listed on the website of the NIST (National Institute of Standards and Technology).²³ For the He-PMP, Cl(I) emission under optimized conditions was strongest at 837.7 nm, which concurred with NIST data. Although Cl(II) emission was expected to show strong intensity in the vacuum region, 107.1 nm and 134.7 nm, no such emission was obser-

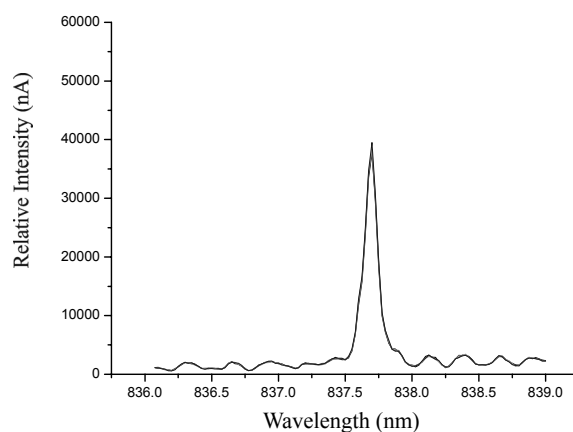


Figure 5. Spectrum of Cl(I) at 837.7nm for 300 $\mu\text{g/mL}$ KCl using the He-PMP.

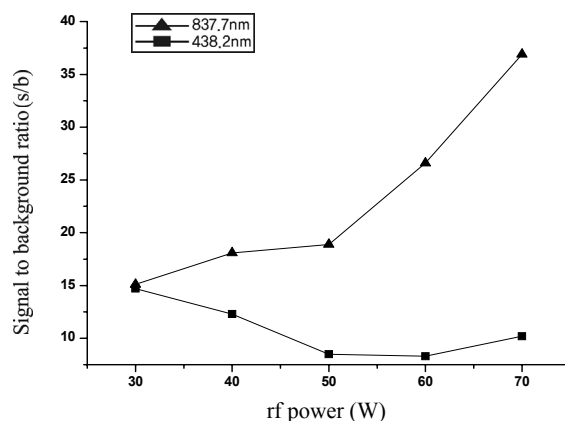


Figure 6. Changes in signal to background ratio (s/b) for Cl (I) lines for the He-PMP system.

ved for our He-PMP system.

The spectrum in the vicinity of the 837.7 nm line is shown in Fig. 5, for a 300 $\mu\text{g/mL}$ KCl control sample. The emission intensities of the peaks were integrated and background contributions were subtracted to obtain net emission intensities for four replicates. During the optimization process, signal to noise ratios were determined when rf power was increased from 30 to 70 W; results are shown in Fig. 6. The two wavelengths of interest showed opposite characters in this respect, i.e., the signal to background (s/b) ratio of the 837.7 nm line increased, whereas that of the 438.2 nm decreased. Noticeably the s/b ratio of the 438.2 nm became smaller than the 837.7 nm as the power increased, probably due to higher background level and higher transition energy required. Although higher sensitivities can be achieved at higher powers, measurements were carried out at 70 W in this experiment due to the sensitivity required for sanitizer analysis and the thermal stability of the PDMS microchip. Using the optimized conditions, the calibration curve of Cl(I) at 837.7 nm was as is shown in Fig. 7. The best attainable detection limit (using the 3σ criterion) and using potassium permanganate as oxidant was found to be 0.81 $\mu\text{g/mL}$, which was sensitive enough to analyze samples containing $\sim 100 \mu\text{g mL}^{-1}$ of chlorine in the form of chlorinated compounds in water.

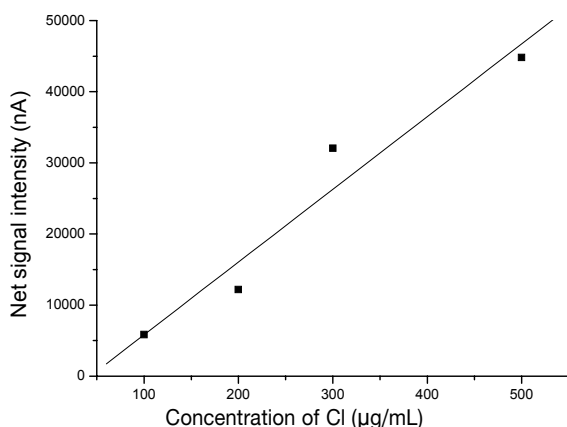


Figure 7. Calibration curve for Cl(I) at 837.7nm.

For the purposes of this study, sanitizing solution was obtained from Duck Young Engineering (Gwachun, Korea), which has developed a prototype electrolysis system for the production of chlorinated water for sanitation purposes in the food and related industries. Chlorinated water was produced by electrolyzing NaCl, and naturally hydrogen gas is produced as a by-product. Sanitizing solutions can contain several types of inorganic chlorine containing compounds, such as, chloride, ClO, and several others, and although sanitization efficiencies were initially expected to be influenced predominantly by compounds like ClO, total chlorine content determinations do in fact provide valuable information related to efficiency. The concentration of total chlorine in sample solutions during the present study were ~4,570 µg/mL and the relative standard deviation of the analysis was 1.40% when the He-PMP emission system was operated under the optimized conditions.

Acknowledgments. This work was supported by Internal Research Fund of Dankook University (2008).

References

- Burnett, A. B.; Iturriaga, M. H.; Escartin, E. F. *J. of Food Protection* **2004**, *67*, 742.
- Kwon, J.-Y.; Kim, B.-S.; Kim, G.-H. *Korean J. of Food Science and Technology* **2006**, *38*, 28.
- Beuchat, L. R. *J. of Food Protection* **1999**, *62*, 845.
- Nakahara, T.; Nishida, T. *Spectrochimica Acta, Part B* **1998**, *53*, 1209.
- Pohl, P.; Zapata, I. J.; Amberger, M. A. *Spectrochimica Acta, Part B* **2008**, *63*, 415.
- Tagami, K.; Uchida, S.; Hirai, I. *Analytica Chimica Acta* **2006**, *570*, 88.
- Bass, A.; Chevalier, C.; Blades, M. W. *J. Anal. At. Spectrom.* **2001**, *16*, 919.
- Rahman, M. M.; Blade, M. W. *Spectrochimica Acta Part B* **1997**, *52*, 1983.
- Sung, Y. I.; Lim, H. B. *J. Anal. At. Spectrom.* **2003**, *18*, 897.
- Bilgic, A. M.; Voges, E.; Engel, U.; Broekaert, J. A. C. *J. Anal. At. Spectrom.* **2000**, *15*, 579.
- Bilgic, A. M.; Engel, U.; Voges, E.; Uckelheim, M. K.; Broekaert, J. A. C. *Plasma Sources Sci. Technol.* **2000**, *9*, 1.
- Iza, F.; Hopwood, J. *Plasma Sources Sci. Technol.* **2002**, *11*, 229.
- Minayeva, O. B.; Hopwood, J. A. *J. Anal. At. Spectrom.* **2002**, *17*, 1103.
- Lim, H. B.; Kim, D.; Jung, T.; Houk, R. S.; Kim, Y. *Analytica Chimica Acta* **2005**, *545*, 119.
- Houk, R. S.; Zhai, Y. *Spectrochimica Acta, Part B* **2001**, *56*, 1055.
- Abdallah, M. H.; Mermet, J. M. *Spectrochimica Acta, Part B* **1982**, *37*, 391.
- Ishii, I.; Montaser, A. *Spectrochimica Acta, Part B* **1991**, *5986*, 1197.
- Sung, Y.-I.; Lim, H. B.; Houk, R. S. *J. Anal. At. Spectrom.* **2002**, *17*, 565.
- Mermet, J. M. *Spectroscopic Diagnostics: Basic Concept in Inductively Coupled Plasma Emission Spectroscopy*; Boumans, P. W. J. M., Ed.; John Wiley & Sons Inc.: NY., 1987; Part 2, Chapter 10, pp 368-372.
- Miro, M.; Estela, J. M.; Cerda, V. *Talanta* **2004**, *63*, 201.
- Oh, J.; Lim, H. B. *Spectrochimica Acta Part B* **2008**, *63*, 1263.
- Ryu, W. K.; Kim, D. H.; Lim, H. B.; Houk, R. S. *Bull. Korean Chem. Soc.* **2007**, *28*, 553.
- NIST website: <http://physics.nist.gov/PhysRefData/Handbook/>.